**Supplementary Data**

# Akt2 functions as a master regulator of all Akt isoforms and promotes resistance to hypoxia by regulating the induction of miR-21 upon oxygen deprivation

Christos Polytarchou [1], Dimitrios Iliopoulos [2,3], Maria Hatziapostolou [1], Filippos Kottakis [1], Ioanna G. Maroulakou [1,4], Kevin Struhl [2], Philip N. Tsichlis [1,*]

[1] Molecular Oncology Research Institute, Tufts Medical Center, Boston, MA

[2] Department of Biological Chemistry and Molecular Pharmacology, Harvard Medical School, Boston, MA.

**Supplementary Figures**

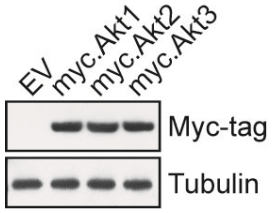


**Figure S1. Spontaneously immortalized TKO lung fibroblasts engineered to express myc-Akt1, myc-Akt2 or myc-Akt3, express equal levels of the three Akt isoforms.**

Immortalized lung fibroblasts were transduced to express different Akt isoforms. Ablation of the endogenous Akt1 by Cre, gave rise to the triple knockout (EV) cells, or triple Akt knockout cells expressing a single Akt isoform at a time. Cell lysates, were probed with anti-Myc and anti-α-tubulin (loading control) antibodies.

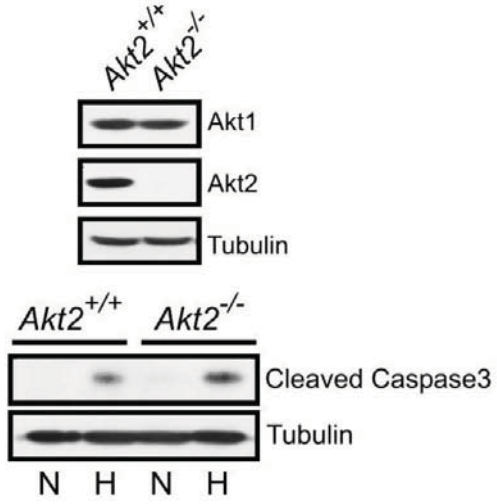


**Figure S2. Akt2 ablation promotes hypoxia-induced apoptosis.**

Cell lysates, harvested 24 hours after exposure of *Akt2*$^{+/+}$ and *Akt2*$^{-/-}$ MEFs to hypoxia were probed with anti-Akt1, anti-Akt2 anti-cleaved caspase-3 and anti-α-tubulin (loading control) antibodies.

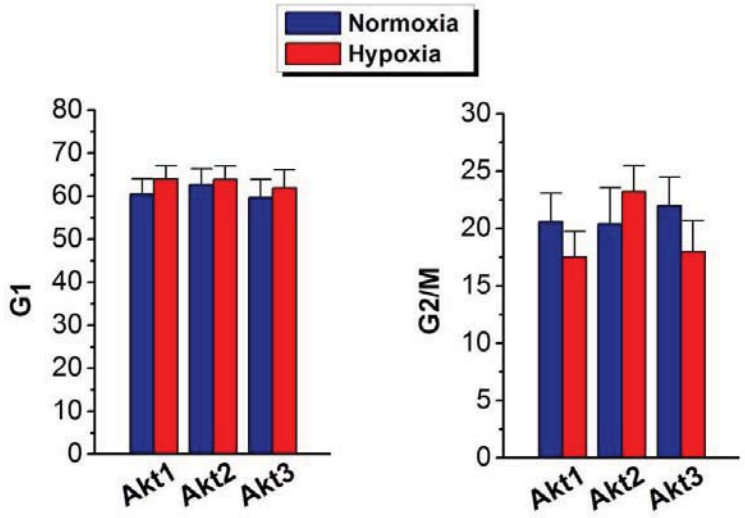


**Figure S3. Cell cycle analysis of Akt1, Akt2 and Akt3-expressing immortalized lung fibroblasts exposed to hypoxia.**

Distribution of the cells shown in figure 1E (*right panel*) in the G1 and G2/M phases of the cell cycle. Their distribution in the S phase was shown in figure 1E.

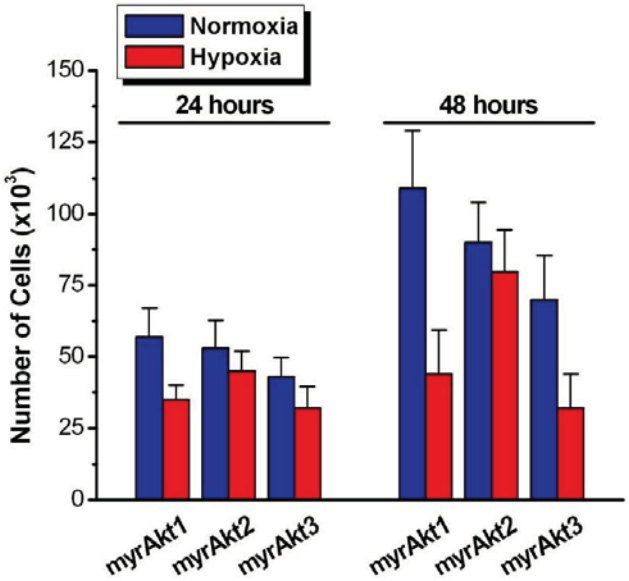


**Figure S4. MyrAkt2, similar to Akt2, selectively protects cells from hypoxia.**

Numbers of MyrAkt1, MyrAkt2, or MyrAkt3-expressing cells surviving under hypoxia. Cells were counted at 24 and 48 hours after exposure to normoxia or hypoxia. Data are expressed as mean ± SD.

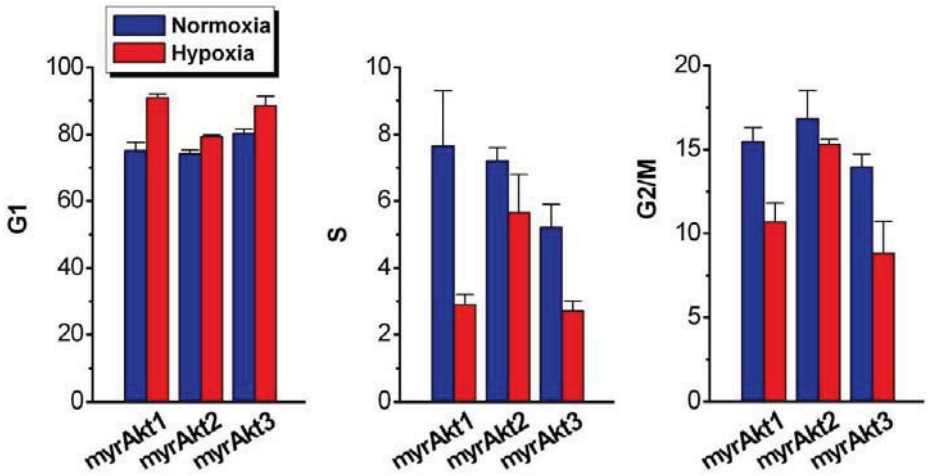


**Figure S5. Cell cycle distribution of MyrAkt1, MyrAkt2, or MyrAkt3-expressing cells exposed to hypoxia.**

Cells growing in normoxia or hypoxia for 24 hours were analyzed for cell cycle distribution. Flow cytometry was performed on ethidium bromide-stained cell nuclei. Cumulative data from two experiments. Data are expressed as mean ± SD.

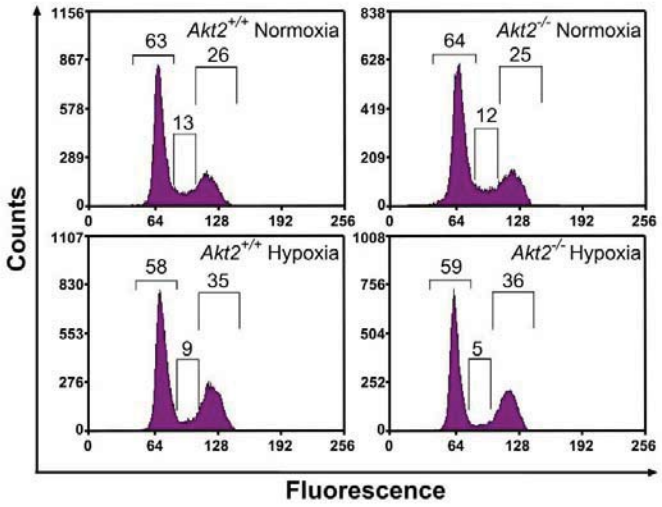


**Figure S6. Cell cycle analysis of *Akt2*$^{-/-}$ and *Akt2*$^{+/+}$ MEFs exposed to hypoxia.**

Flow cytometry was performed on ethidium bromide-stained cell nuclei, 24 hours after exposure to hypoxia.

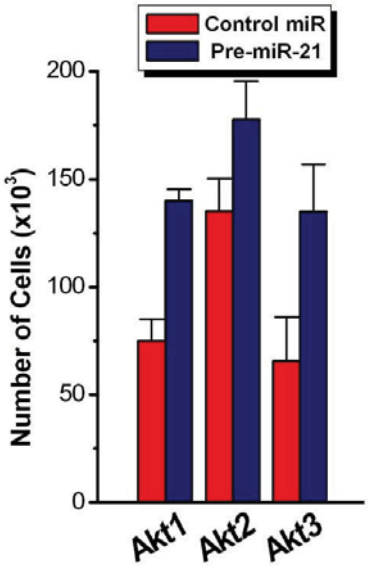


**Figure S7. Pre-miR-21 confers resistance to hypoxia in Akt1 and Akt3-expressing cells.**

Cells were transfected with control miR, or pre-miR-21 and they were counted after they were cultured in normoxia or hypoxia for 48 hours. Data are expressed as mean ± SD.

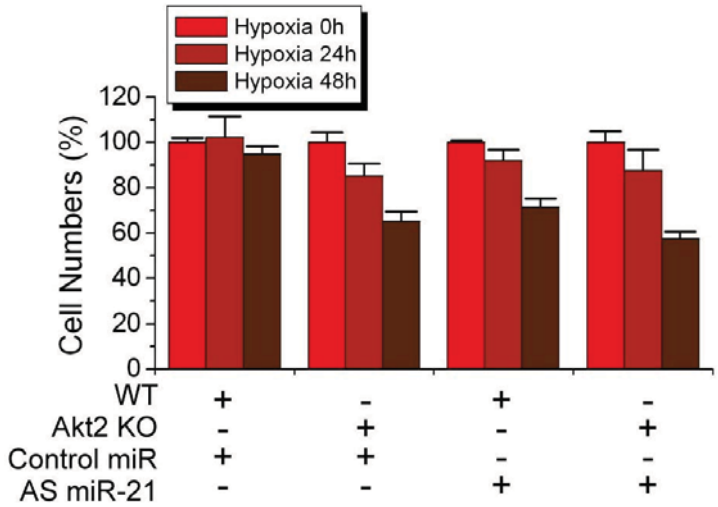


**Figure S8. Anti-miR-21 renders wild type MEFs sensitive to hypoxia.**

Cells were transfected with control miR, or anti-sense-miR-21, as indicated, and they were counted after they were cultured in hypoxia for 0, 24 and 48 hours. Data are expressed as mean ± SD.

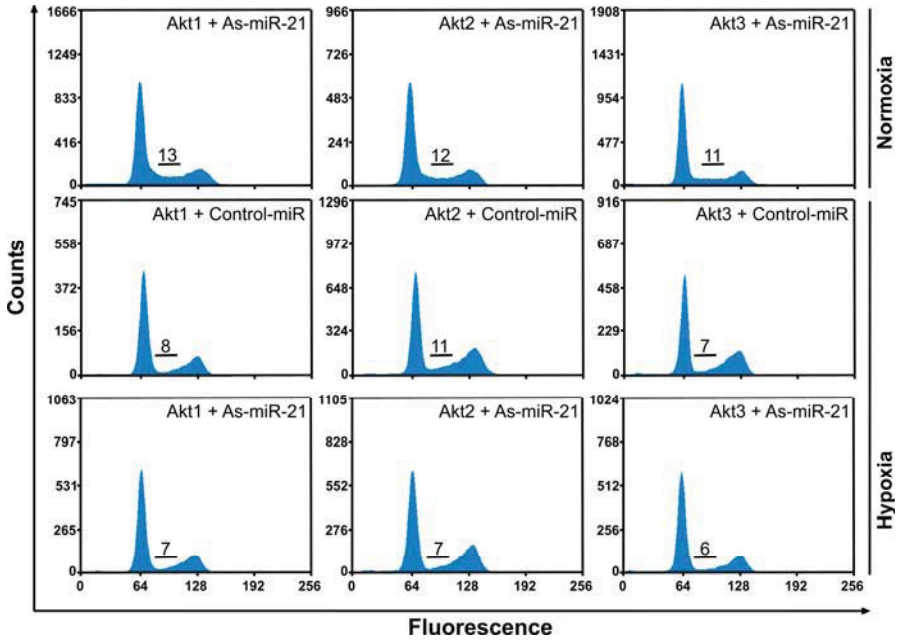


**Figure S9. Cell cycle distribution of Akt1, Akt2 and Akt3-expressing immortalized lung fibroblasts transfected with anti-miR-21 and grown in normoxia or hypoxia.**

Cells were transfected with anti-miR-21 and they were cultured in normoxia or hypoxia for 24 hours. Cell nuclei were stained with ethidium bromide and they were analyzed by flow cytometry. Akt2-expressing cultures exposed to hypoxia contain a higher percentage of cells in S phase than Akt1 and Akt3-expressing cultures, exposed to hypoxia. As-miR-21 obliterates the difference between Akt1, Akt2 and Akt3-expressing cells exposed to hypoxia.

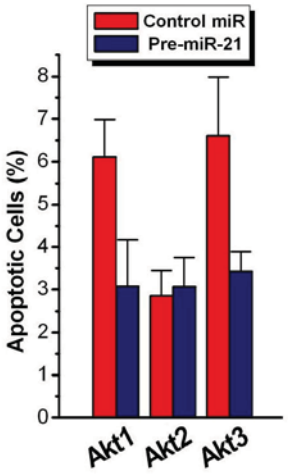


**Figure S10. Pre-miR-21 protects Akt1 and Akt3-expressing cells from hypoxia-induced apoptosis.**

TUNEL assay was performed on cells transfected with control miR, or pre-miR-21 and cultured in normoxia or hypoxia for 24 hours. Cumulative data from two experiments. Data are expressed as mean ± SD.

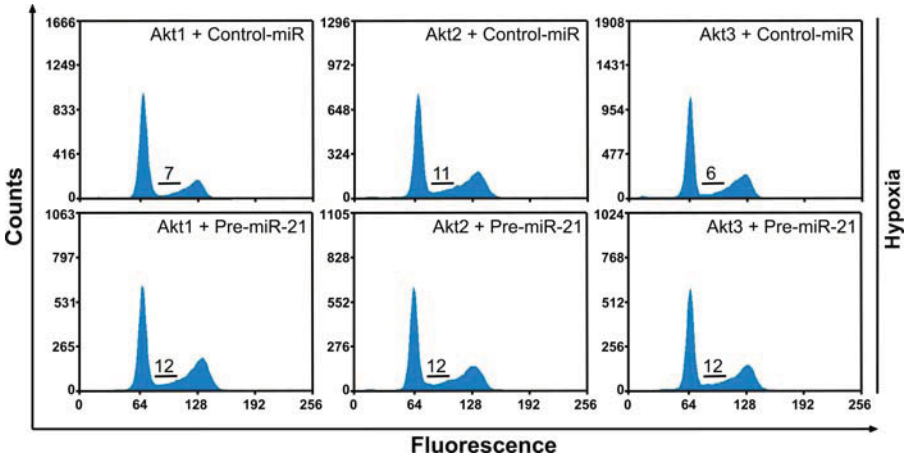


**Figure S11. Cell cycle distribution of Akt1, Akt2 and Akt3-expressing immortalized lung fibroblasts transfected with control miR or pre-miR-21 and grown in hypoxia.**

Cells were transfected with control miR or pre-miR-21 and they were cultured in hypoxia for 24 hours. Cell nuclei were stained with ethidium bromide and they were analyzed by flow cytometry. Pre-miR-21 increases the percentage of S phase cells in Akt1- and Akt3-expressing cultures exposed to hypoxia to levels similar to the ones in Akt2-expressing cultures.

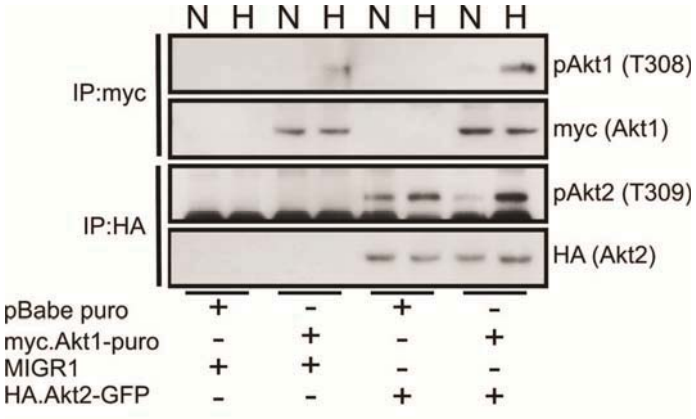


**Figure S12. The Akt2/miR-21/PTEN pathway is a master regulator of all Akt isoforms in cells growing in hypoxia.**

*Akt1*$^{fl/fl}$*/Akt2*$^{-/-}$*/Akt3*$^{-/-}$ immortalized lung fibronblasts were transduced with retroviral constructs of myc-Akt1, HA-Akt2 or mycAkt1 and HA-Akt2. The endogenous floxed Akt1 was subsequently ablated with Cre. The phosphorylation of myc-Akt1 and HA-Akt2 in the three cell lines, before and after exposure to hypoxia was addressed by probing anti-myc and anti-HA immunoprecipitates with the phosphor-Akt (Thr308) antibody. To monitor the efficiency of the IP, the same immunoprecipitates were probed with the anti-myc and the anti-HA antibodies.

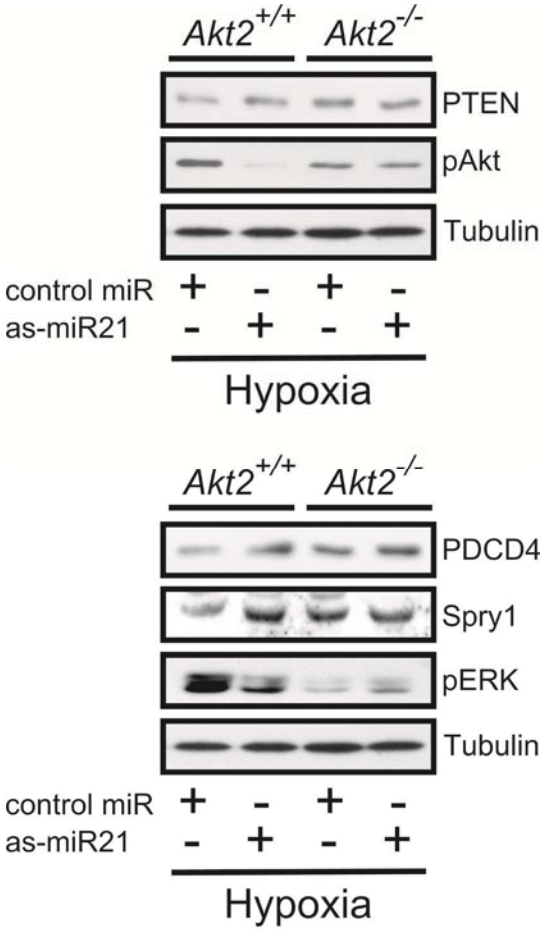


**Figure S13. Anti-miR-21 upregulates PTEN, PDCD4 and Spry1, in *Akt2*$^{+/+}$, but not in *Akt2*$^{-/-}$ cells, growing in hypoxia.**

*Upper panel*: Anti-miR-21 upregulates PTEN and inhibits Akt phosphorylation in *Akt2*$^{+/+}$ but not in *Akt2*$^{-/-}$ MEFs growing in hypoxia. *Akt2*$^{+/+}$ and *Akt2*$^{-/-}$ MEFs were transfected with control miR or anti-miR-21. Cell lysates harvested after 24 hours of growth in hypoxia, were probed with the indicated antibodies.

*Lower panel*: Anti-miR-21 upregulates PDCD4 and Spry1 and inhibits ERK phosphorylation in *Akt2*$^{+/+}$ but not in *Akt2*$^{-/-}$ MEFs growing in hypoxia. *Akt2*$^{+/+}$ and *Akt2*$^{-/-}$ MEFs were transfected with control miR or anti-miR-21. Cell lysates harvested after 24 hours of growth in hypoxia, were probed with the indicated antibodies.

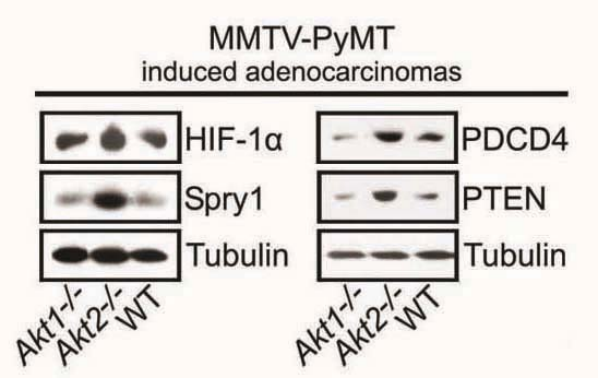


**Figure S14. The Akt2-miR21 pathway is active in hypoxic tumors in mice.**

Representative western blots of tumor cell lysates derived from tumors arising in MMTV-PyMT/*Akt1*$^{-/-}$, MMTV-PyMT/*Akt2*$^{-/-}$ and MMTV-PyMT/wild type mice was probed with the indicated antibodies.

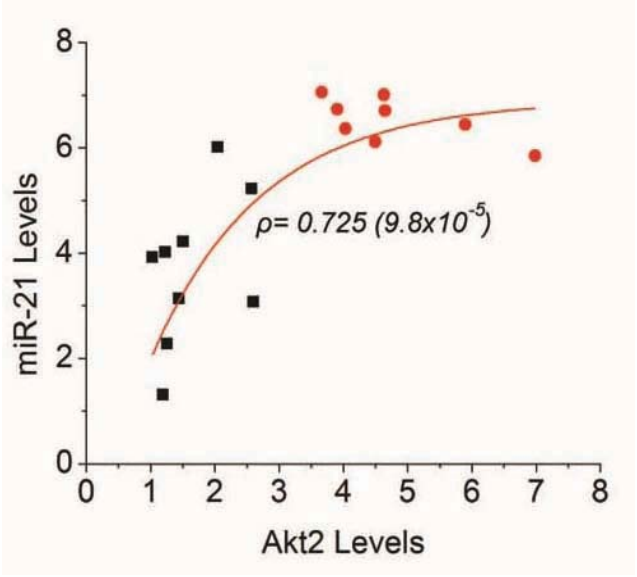


**Figure S15. The Akt2-miR21 pathway is active in ovarian carcinomas.**

Positive correlation between the expression of Akt2 and miR-21 in HIF-1α-positive (hypoxic) ovarian carcinomas. MiR-21 and HIF-1α levels were measured by real time RT-PCR. Spearman rank correlation and *P*-value in parenthesis are shown. (●) Tumors expressing high levels of Akt2; (■) Tumors expressing low levels of Akt2.

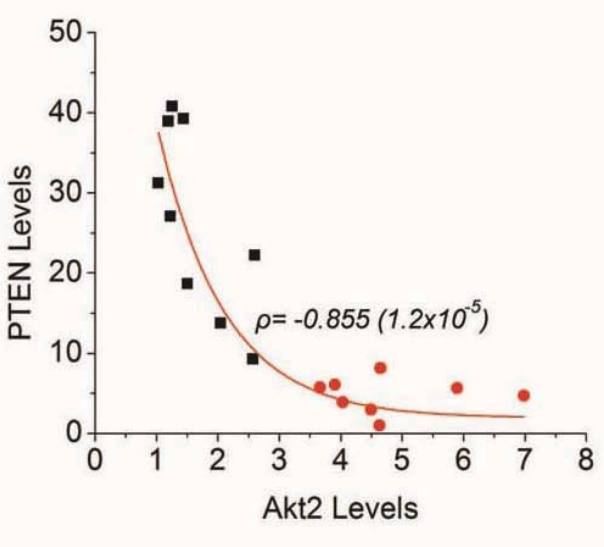


**Figure S16. The Akt2-miR21 pathway is active in ovarian carcinomas.**

Negative correlation between the expression of Akt2 and PTEN in HIF-1α-positive (hypoxic) ovarian carcinomas. PTEN and HIF-1α levels were measured by real time RT-PCR. Spearman rank correlation and *P*-value in parenthesis are shown. (●) Tumors expressing high levels of Akt2; (■) Tumors expressing low levels of Akt2.

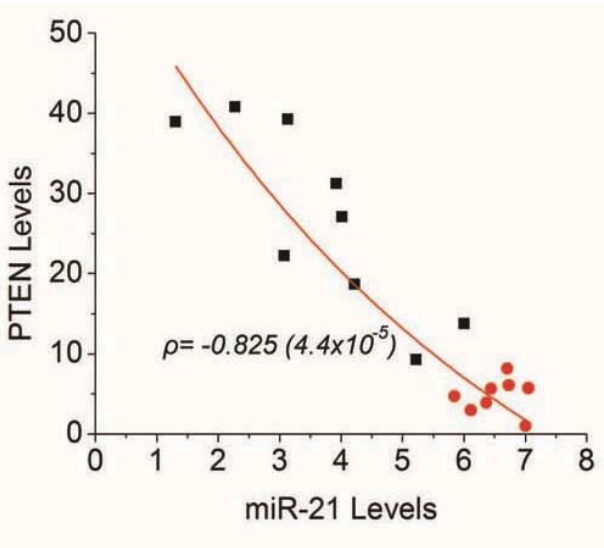


**Figure S17. The Akt2-miR21 pathway is active in ovarian carcinomas.**

MiR-21 and PTEN levels exhibit a negative correlation confirming the regulation of PTEN by miR-21. Spearman rank correlation and *P*-value in parenthesis are shown. Hypoxic

tumors expressing high levels of Akt2 (●), also express high levels of miR-21 and low levels of PTEN.

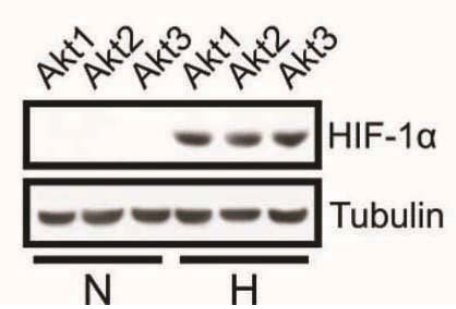


**Figure S18. The level of induction of HIF-1α during hypoxia in cells expressing Akt1, Akt2 or Akt3 is similar.**

Akt1, Akt2 and Akt3-expressing immortalized lung fibroblasts were exposed to hypoxia. Cell lysates harvested 24 hours later, were probed with the indicated antibodies.

**Supplementary Methods**

**Cell culture, retroviral and lentiviral infections.**

Mouse lung fibroblasts from *Akt1*$^{fl/fl}$/*Akt2*$^{-/-}$/*Akt3*$^{-/-}$ mice were cultured in DMEM supplemented with 10% fetal bovine serum (FBS), penicillin and streptomycin, sodium pyruvate, nonessential amino acids and glutamine. Passage of these cells every three to four days led to the establishment of spontaneously immortalized cell lines. Established cell lines were cultured in the same media, under standard culture conditions.

Wild-type Akt1, Akt2 and Akt3, tagged with the myc epitope at their C-terminus, were cloned in the retroviral vector pMigR1-GFP. Retrovirus constructs were packaged in 293T cells transiently transfected with these constructs and with EcoPac, an ecotropic virus packaging construct, using Fugene 6 (11814443001, Roche). Immortalized lung fibroblasts were infected with the packaged viruses as follows: Cells were pre-treated with DEAE dextran (25 μg/ml). Forty five minutes later, they were washed and overlayed with virus-containing media. Infected cells were sorted for GFP 48 hours later. Cells generated from three independent infections for each retroviral construct, were analyzed for Akt isoform expression by probing their lysates with the respective antibodies. To abolish the expression of the endogenous Akt1, cells were super-infected with a MigR1-RFP-based retroviral construct of the Cre recombinase and they were sorted 48 hours later. Ablation of endogenous *Akt1* by Cre, gave rise to Akt-null cells (TKO) or triple Akt knockout cells expressing a single Akt isoform at a time.

The tumor cell lines OVCAR3, SKOV3, PEO1, PEO4, 1847, OVCAR4 and MDA-MB 231 were cultured in RPMI-1640 supplemented with 10% fetal bovine serum (FBS), penicillin, streptomycin and glutamine.

ShRNAs against Akt1 or Akt2 were cloned in the lentiviral vector pLKO.1. Lentiviral constructs of shAkt1 and shAkt2 were packaged in 293T cells transiently transfected with these constructs and with pCMV-VSVG and pCMV-dR8.2 dvpr. Cancer cell lines were infected with the packaged viruses in the presence of 10 μg/ml Polybrene (Sigma). Infected cells were selected for puromycin (Sigma) resistance (2 μg/ml). Knockdown efficiency was tested by probing their lysates with anti-Akt1 and anti-Akt2 antibodies.

**Hypoxia, TUNEL assay, and cell cycle analysis.**

Cells were cultured under 0.2% $O_2$, 5% $CO_2$ (hypoxia) in an in vivo$_2$ Hypoxia Workstation equipped with a Ruskinn hypoxia gas mixer. Live cells were measured by direct counting, using a standard hemocytometer. Apoptosis was monitored using a terminal deoxynucleotidyltransferase biotin-dUTP nick end labeling (TUNEL) kit (11684795910, Roche). Cell cycle distribution was monitored as previously described (*1*). Briefly, cells cultured in hypoxia and normoxia were scrapped, pelleted at 1,000 g at 4°C for 5 min, resuspended at $10^6$ cells/ml and lysed in lysis-staining buffer (3.4 mM sodium citrate, 10 mM NaCl, 0.1% Nonidet P-40, 75 μM ethidium bromide [EtBr]) on ice. The fluorescence intensity of cell nuclei was measured by flowcytometry (FACS).

**Real-time RT-PCR Analysis**

Real-time RT-PCR was performed to determine the expression levels of miR-21 in cells cultured in normoxia and hypoxia, in murine PyMT-induced mammary adenocarcinomas and in human ovarian carcinomas. The RNA of cultured cells and of murine mammary adenocarcinomas was isolated, using the mirVana miRNA isolation kit (AM1561, Ambion), while the RNA of human ovarian carcinomas was purchased from commercial sources (see below). Reverse Transcription was carried out using the First-strand cDNA synthesis kit (201100) and primer sets for miR-21 (202007) and U6 snRNA (201510).

Real-time PCR was carried out in dublicate using the SYBR Green master mix (201000, Exiqon) on an Opticon2 PCR instrument (Biorad). miR-21 expression levels were normalized to the levels of RNU44 (RNA from human ovarian carcinomas) or U6 small nuclear RNA (RNA from all other sources) (internal controls).

Real time RT-PCR for HIF-1α (5'-CGTTCCTTCGATCAGTTGTC-3' and 5'-TCAGTGGTGGCAGTGGTAGT-3'), PTEN (5'-CCGAAAGGTTTTGCTACCATTCT-3' and 5'-AAAATTATTTCCTTTCTGAGCATTCC-3') and AKT2 (5'-CCATGAATGAGGTGTCTGTCA-3' and 5'-GGCCTCCAGGTCTTGATGTA-3') was carried out in RNAs from 31 ovarian adenocarcinomas using SYBR Green mastermix (170-8882, Bio-rad) and a 7900HT Applied Biosystems PCR machine. Glyceraldehyde-3-phosphate dehydrogenase (GAPDH) (5'-CGCTCTCTGCTCCTCCTGTT-3' and 5'-CCATGGTGTCTGAGCGATG-3') was used as the internal control.

**Immunoprecipitation and Immunoblotting**

Experiments in this report utilized the following antibodies from Cell Signaling Technologies: anti-myc-tag (# 2276), anti-HA-tag (#2367), anti-Akt1 (#2938), anti-Akt2 (#2964), anti-Akt3 (#3788), anti-phospho-Akt (Thr308) (#4056), anti-phospho-Akt (Ser473) (#4060), anti-phospho-Akt Substrate (RXRXXS/T) (#9614), anti-phospho-GSK-3-alpha/beta (Ser21/9) (#9331), anti-phospho-4E-BP1 (Thr70) (#9455), anti-phospho-mTOR (Ser2448) (#2971), anti-phospho-p44/42 MAPK (Thr202/Tyr204) (#9101), anti-phospho-CREB (Ser133) (#9198), anti-PTEN (#9559), anti-PDCD4 (#9535), anti-Cleaved Caspase-3 (Asp175) (#9664), anti-CREB (#9104). Alternatively, they utilized the anti-Spry1 antibody sc-30048 (Santa Cruz Biotechnology), the anti-HIF-1α antibody MAB1536 (R&D Systems) or the anti-tubulin antibody T5168 (Sigma).

For western blotting, cells were lysed on ice, using a Triton X-100 lysis buffer (50 mM Tris, pH 7.5, 150 mM NaCl, 1 mM EDTA, 1mM EGTA, 1% Triton X-100, 2.5 mM sodium orthovanadate, 1 mM phenylmethylsulfonyl fluoride, 50 mM NaF, 10 μg/ml leupeptin, and 5 μg/ml aprotinin). Twenty micrograms of total protein from each sample were resolved in a 10% SDS-PAGE and transferred to PVDF membranes.

For the immunoprecipitation of individual proteins from total cell lysates, anti-myc-tag or anti-HA antibody beads (E6779, Sigma) were mixed with the lysates under continuous agitation overnight, at 4$^{o}$C. Protein G agarose beads (15920-010, Invitrogen) were then added to the anti-myc-tag immunoprecipitates for 1h under agitation at 4$^{o}$C. Beads were subsequently washed 5 times in lysis buffer and boiled in sample buffer. Proteins released in the buffer were resolved in a 10% SDS-PAGE, transferred to PVDF membranes and probed with the indicated antibodies.

**Identification of transcription factor binding motifs in the miR-21 promoter/enhancer**

Three selection criteria were used sequentially to identify transcription factor binding motifs in the miR-21 promoter (*2*): 1) The Lever algorithm was first applied to assess the potential enrichment of a given motif in cis-regulatory modules (CRMs), in the non-coding sequences flanking known genes (*3*); 2) the phylogenetic conservation of the binding motifs identified with the use of the Lever algorithm was addressed next. Conservation was evaluated with the PhylCRM algorithm, across 12 different mammalian species (mouse, rat, human, rabbit, chimp, macaque, cow, dog, armadillo, tenrec, opossum and elephant). Only binding sites with a high conservation score (higher than 200) were selected. 3) Finally, the nucleosome occupancy in the conserved binding sites was visually evaluated, using the UCSC genome browser track. The top

transcription factor binding motifs identified in miR-21 promoter with the methodology outlined above were two CREB motifs (motif 1: chr17:55269873-55269880 and motif 2: chr17:55273384-55273391) and one NF-κB binding motif (chr17:55,272,131-55,272,140).

**In vitro mutagenesis of the miR-21 promoter in the Luciferase Reporter Construct.**

To introduce point mutations in the two CREB binding sites and the one NF-κB binding site in the miR-21 promoter, the miR-21pro4,6-Luc reporter construct was mutagenized by oligonucleotide-directed mutagenesis with the Quik-ChangeII Site-Directed Mutagenesis Kit (200524-5, Stratagene). After the annealing of the mutagenesis primers, the two DNA strands were completed with Pfu Turbo DNA polymerase, and the parental double-stranded DNA was digested by DpnI. The digested DNA was transformed into XL1-Blue super competent bacteria. Mutant clones were verified by DNA sequence analysis.

**Chromatin Immunoprecipitation**

Chromatin immunoprecipitation was carried out as described previously (*4*). Immunoprecipitated DNA was extracted with the Qiagen Purification Kit (Qiagen, MD, USA). The samples were analyzed by real-time PCR, using the following primer pairs (CREB site 1: GCCTCCCAAGTTTGCTAATG and CTGACTTGTCCCCTCTTCTCA; CREB site 2: TGGGGTTCGATCTTAACAGG and CTGATAAGCTACCCGACAAGG; NF-KB site: AAATTGGGAGGACTCCAAGC and AGGCCAGTCTGTTGCAAGTT; H3-K9ac site: CCATGAAAGGATTCAAAGTTCA and GGGCGGTCTTTCTCAATCTA). Primers for H3-K9Ac were designed around the CREB1 binding site.

### *In situ* microRNA hybridization

Mircury LNA Detection probes for the detection of mmu-miR-21 by *in situ* hybridization, 5'-end labeled with 56-FAM (39103-04, Exiqon) were used as previously described with minor modifications (*5*). Sections of mammary adenocarcinomas arising in MMTV-PyMT/WT, MMTV-PyMT/*Akt1*$^{-/-}$ and MMTV-PyMT/*Akt2*$^{-/-}$ mice (5 μm-thin) were deparaffinized with xylene (2x40 min incubations with gentle shaking on a 50 rpm shaker), followed by treatment with serial dilutions of ethanol (100%, 100%, 75%, 50% and 25%) (5 min each) and by two changes of DEPC-dd$H_2O$. Slides were then submerged for 5 min in 0.2 N HCl, washed with DEPC-PBS, digested with proteinase K (40 μg/ml) for 45 min at 25$^{o}$C, rinsed with 0.2% glycine/DEPC-PBS and 3XDEPC-PBS and postfixed with 4% formaldehyde in PBS for 10 min. Sections were then rinsed twice with DEPC-PBS, treated with acetylation buffer (300 μl acetic anhydride, 670 μl triethanolamine, 250 μl of 12 N HCl per 48 ml dd$H_2O$) and rinsed with DEPC-PBS (x4) and with 5xSSC (x2). Sections were then pre-hybridized at 51$^{o}$C for 2 hrs in hybridization buffer (50% formamide, 5xSSC, 0.1% Tween-20, adjusted to pH 6.0 with 9.2 mM citric acid, 50 μg/ml heparin, 500 μg/ml yeast tRNA) in a humidified chamber (50% formamide, 5xSSC). Following pre-hybridization, sections were hybridized overnight to the DNA probe (20 nM in pre-warmed hybridization buffer) in a humidified chamber, at 51$^{o}$C. Following hybridization, sections were rinsed twice with 5xSSC, three times, 20 min each, with 50% formamide/2xSSC at 51$^{o}$C and five times with PBS/0.1% Tween-20 (PBST). At the end, sections were mounted with coverslips in DAPI-containing (Vector Labs) Vectashield mounting medium. Images were captured with a Nikon Eclipse 80i microscope and a Spot charge-coupled device camera (Diagnostic Instruments). All images were captured and processed using identical settings.

**Immunohistochemistry**

Sections of the mammary adenocarcinomas described above were deparaffinised with xylene (3x5 min incubations) followed by treatment with serial dilution of ethanol (100%, 100%, 95% and 95%, 10 min each) and by two changes of $ddH_2O$. Antigen unmasking was achieved by boiling the slides (95-99$^oC$) for 10 min, in 10 mM sodium citrate, pH 6.0. Sections were then rinsed three times with $ddH_2O$, immersed in 3% $H_2O_2$ for 10 minutes, washed twice with $ddH_2O$ and once with TBST (TBS, 0.1% Tween-20) and blocked for one hr with blocking solution (5% normal goat serum in TBST). HIF-1α and PTEN antibodies were diluted in blocking solution (1:200 and 1:100, respectively) and incubated with the sections overnight at 4$^oC$. Following incubation with the antibodies, sections were washed three times, five min each, with TBST and incubated for one hr at room temperature with HRP-labelled anti-mouse or anti-rabbit antibodies diluted in blocking solution (1:500). Sections were finally washed three times, five min each, with TBST, stained with the DAB substrate kit for peroxidase (SK-4100, Vector Laboratories), dehydrated and mounted in Cytoseal XYL (8312-4, Richard-Allan Scientific).

**Supplementary References**

1. Polytarchou C, Pfau R, Hatziapostolou M, Tsichlis PN. The JmjC domain histone demethylase Ndy1 regulates redox homeostasis and protects cells from oxidative stress. Mol Cell Biol. 2008;28:7451-64.

2. Ozsolak F, Poling LL, Wang Z, Liu H, Liu XS, Roeder RG, et al. Chromatin structure analyses identify miRNA promoters. Genes Dev. 2008;22:3172-83.

3. Warner JB, Philippakis AA, Jaeger SA, He FS, Lin J, Bulyk ML. Systematic identification of mammalian regulatory motifs' target genes and functions. Nat Methods. 2008;5:347-53.

4. Iliopoulos D, Hirsch HA, Struhl K. An epigenetic switch involving NF-kappaB, Lin28, Let-7 MicroRNA, and IL6 links inflammation to cell transformation. Cell. 2009;139:693-706.

5. Iliopoulos D, Polytarchou C, Hatziapostolou M, Kottakis F, Maroulakou IG, Struhl K, et al. MicroRNAs differentially regulated by Akt isoforms control EMT and stem cell renewal in cancer cells. Sci Signal. 2009;2:ra62.